APPLICATION OF GRANULATED BLAST FURNACE SLAG TO THE EARTHQUAKE RESISTANT EARTH STRUCTURE AS A GEO-MATERIAL

Hiroshi MATSUDA[1], Haruhiko SHINOZAKI[2], Ryohei ISHIKURA[3] and Naoyoshi KITAYAMA[4]

[1] *Professor, Graduate School of Science and Engineering, Yamaguchi University, Japan*
[2] *Manager, Div. of Civil Engineering, Nippon Steel Corporation, Chiba, Japan*
[3] *Assistant Professor, Graduate School of Science and Engineering, Yamaguchi University, Japan*
[4] *Director of Research laboratory, Fukken CO., LTD, Hiroshima, Japan*
Email: hmatsuda@yamaguchi-u.ac.jp

ABSTRACT:
Granulated Blast Furnace Slag (GBFS) is expected to be useful as a liquefaction-resistant geo-material because GBFS increases in shear strength with time in the ordinary natural wet condition. In this paper, in order to clarify the cyclic shear strength of GBFS for a different stage of hardening, the static shear tests and cyclic un-drained tri-axial tests were carried out for specimens cured in the laboratory and in the field. As a result, it is observed that the cyclic shear strength increases proportionally with static shear strength and specimens with unconfined shear strength over 50kN/m^2 collapse showing a tension crack on its surface in the cyclic tri-axial test.

KEYWORDS:
granulated blast furnace slag, hydraulic property, liquefaction, shear strength

1. BACKGROUND

Iron and steel slag is a by-product in the process of making iron and steel. Blast furnace slag, which is especially a by-product when making pig iron, is included in the classification of iron and steel slag and the manufacturing amount in Japan is about 38.6 million ton in fiscal 2006. Blast Furnace Slag is, furthermore, classified into a granulated blast furnace slag and an air-cooled blast furnace slag. Granulated blast furnace slag (hereinafter referred to as “GBFS” in this paper) is produced by quenching molten furnace slag with high-pressurized water.

GBFS is now used mainly as a raw material for Portland blast furnace cement in Japan. On the other hand, GBFS has useful geo-technical properties such as lightweight, high internal friction angle and high permeability etc., so it is used as a material for backfilling of quay-wall, sand mat and lightweight embankment etc. For these utilizations in the field of civil engineering works, some technical guidelines or standards have already been published.

Furthermore, since GBFS has a hydraulic property by which its shear strength increases with time in the ordinary wet condition without adding any cement-like materials, GBFS is expected to be useful geo-materials against liquefaction. For using GBFS as a liquefaction-resistance material in port and harbor facilities, following technical standards or criteria are shown.

1) GBFS would solidify in about 6 months after construction when used as a backfill material. Then, GBFS is satisfied as a non-liquefied material.
2) When GBFS is not solidified, GBFS is dealt as a granular material or the safety for the liquefaction should be confirmed.

In spite of these standards, the criteria for confirming the level of solidification have not been clarified.

In this paper, in order to clarify the cyclic shear strength in the process of hardening, the static shear tests and

cyclic un-drained tri-axial tests were performed for specimens with different relative densities which are still under hardening process.

2. MATERIALS AND EXPERIMENTAL METHOD

In this study, two samples GBFS-A and GBFS-B which were produced in the different year but in the same manufacturing plant. Table 1 and Fig.1 show the physical properties and grain size distribution curves for samples used in this study. For specimens which are still under granular condition, a saturated sample was poured into the tri-axial testing mold by controlling a relative density as Dr=50% or Dr=80%. To prepare the specimens having a different shear strength which increases with time due to hydraulic property, specimens were compacted in the mold (D=50mm, H=100mm) to a relative density as Dr=50% and Dr=80% and cured in the highly alkalized water of pH=12 by adding the calcium hydrate to tap water. Then, the water temperature was controlled as 80℃ in order to accelerate the hardening. To clarify the effect of high temperature and high alkalization, the specimens for GBFS-B were also cured in the tap water without adding anything and under the room temperature condition.

Table 1 Physical properties of sample.

Materials	Specific Gravity (g/cm^3)	Maximum void ratio	Minimum void ratio
GBFS A	2.695	1.302	0.844
GBFS B	2.643	1.510	1.033

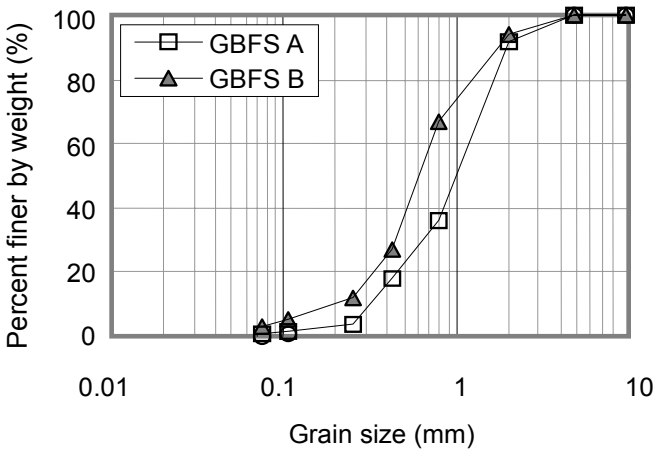

Figure 1 Grain size distribution curve of samples.

For these specimens, three types of shear tests, i.e. consolidated and drained tri-axial compression tests (static tri-axial test), unconfined compression tests and the un-drained cyclic tri-axial tests (cyclic tri-axial test) were performed. In cyclic tri-axial tests and also in static tri-axial tests, all specimens were saturated, where the saturation of specimen was confirmed by measuring the coefficient of pore-water pressure B-value to be over 0.95. When B-value is smaller than 0.95, which is especially seen in hardened specimens, after setting up the specimen in the tri-axial test apparatus, the carbon dioxide was circulated through specimens by controlling the pressures inside the specimen and the tri-axial cell. The static tri-axial tests were performed under the consolidation pressure of 50kPa, 100kPa, 200kPa and the cyclic tri-axial tests were also carried out under 100kPa. The back pressure of 100kPa was applied to the specimen in both static and cyclic tri-axial tests.

In the static tri-axial tests and the unconfined compression tests, the axial load was applied to the specimen by controlling the rate of axial strain as 3%/min and 1%/min, respectively. In the cyclic tri-axial tests, the axial load was applied to the specimen cyclically under the stress-controlled loading condition, in which the loading wave form was sinusoidal and the loading period was set as T=10s.

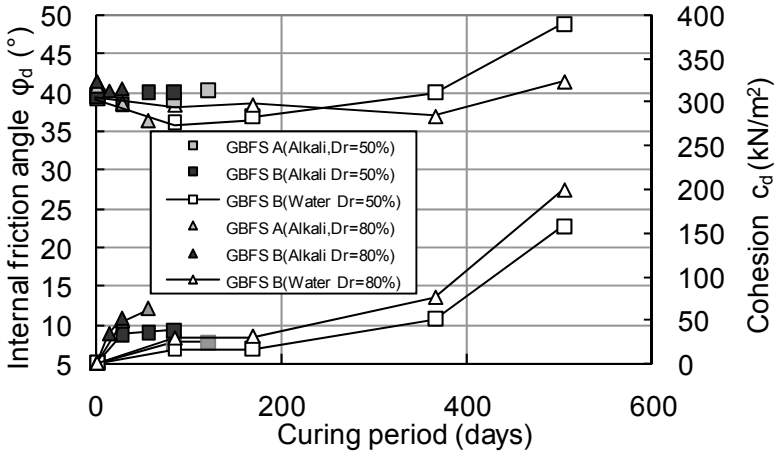

Fig 2 Changes in the angle of shear resistance ϕ_d and cohesion c_d with elapsed time.

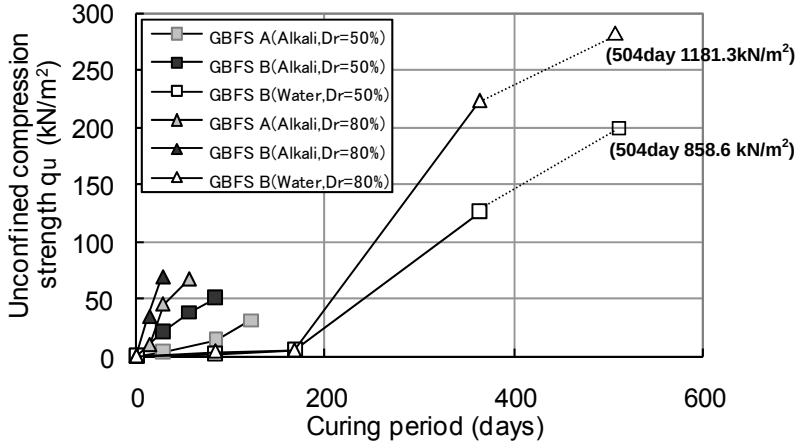

Figure 3 Changes in the unconfined compression strength q_u with curing period.

By the static tri-axial tests and the unconfined compression tests for the specimen with different curing periods, the angle of shear resistance φ_d and the cohesion c_d were obtained. Fig.2 and Fig.3 show relationships between φ_d, c_d, q_u and curing period. φ_d, c_d, and q_u for GBFS-B are greater than those of GBFS-A. In Fig.3, the effects of high alkali and high temperature are shown. As mentioned above, for the sample GBFS-B, specimens were cured in the high alkali and high temperature condition or in the tap water with ordinary room temperature. In the case of Dr=50%, the unconfined shear strength q_u for specimens which were cured for 84 days in the high alkali water with pH=12 and the temperature 80℃, corresponds to those cured for 168-365 days in tap water and in the case of Dr=80%, the curing period of 28 days for high alkali and high temperature water, corresponds to 168-365 days in the normal condition.

3. EFFECTS OF INCREASE IN CYCLIC SHEAR STRENGTH ON LIQUEFACTION RESISTANCE

3.1. Cyclic un-drained tri-axial tests

Figs.4, 5, 6 and 7 show the recorded wave forms for the excess pore water pressure u, cyclic shear stress σ_d, axial strain and effective stress path, on the specimen without a curing in the water (Fig.4), the specimen cured in tap water for 168 days (Fig.5), the specimen cured in tap water for 365 days (Fig.6) and the specimen cured in the high alkali water for 28 days (Fig.7), respectively.

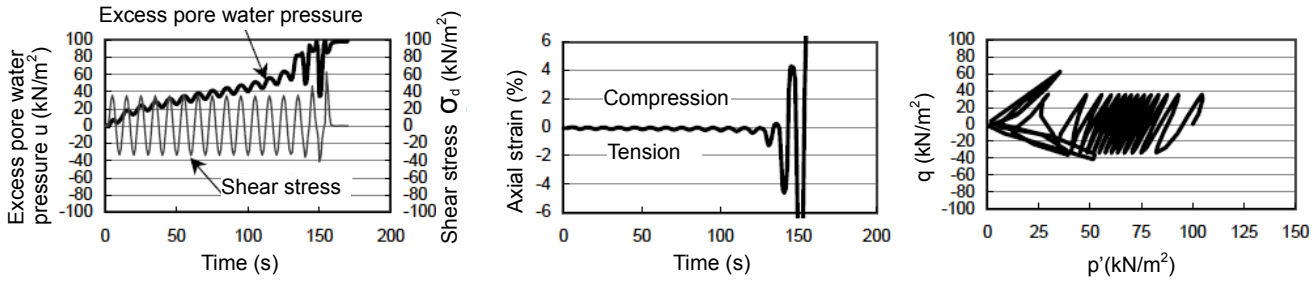

Figure 4 Recorded wave forms for excess pore water pressure, shear stress, axial strain and stress path. (Sample=GBFS B, Dr=50%, $\sigma_d/2\sigma_c$ =0.19, φ_d =39.0°)

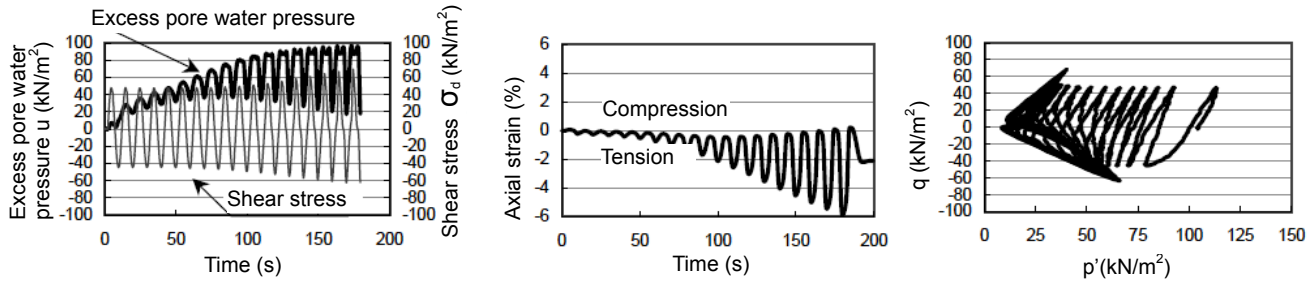

Figure 5 Recorded wave forms for excess pore water pressure, shear stress, axial strain and stress path. (Sample=GBFS B, Dr=50%, $\sigma_d/2\sigma_c$ =0.25, φ_d =36.8°, q_u=5.2kN/m^2, CP=168 days in tap water).

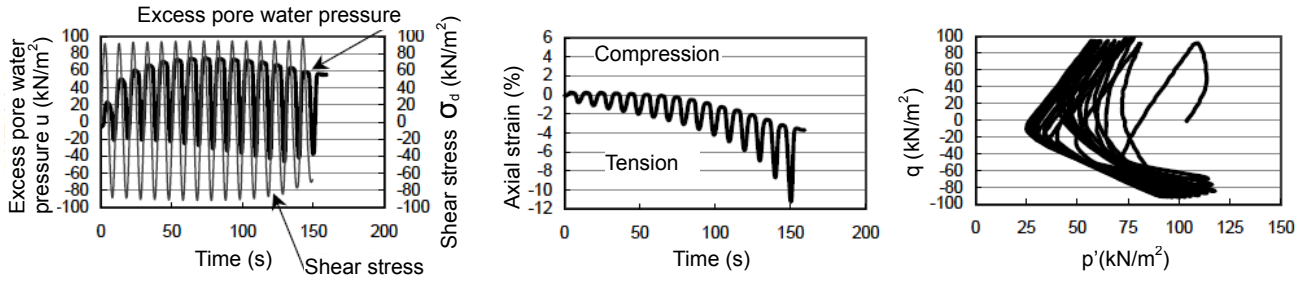

Figure 6 Recorded wave forms for excess pore water pressure, shear stress, axial strain and stress path. (Sample=GBFS B, Dr=50%, $\sigma_d/2\sigma_c$=0.50, φ_d=40.0°, q_u=126.5kN/m^2, CP=365 days in tap

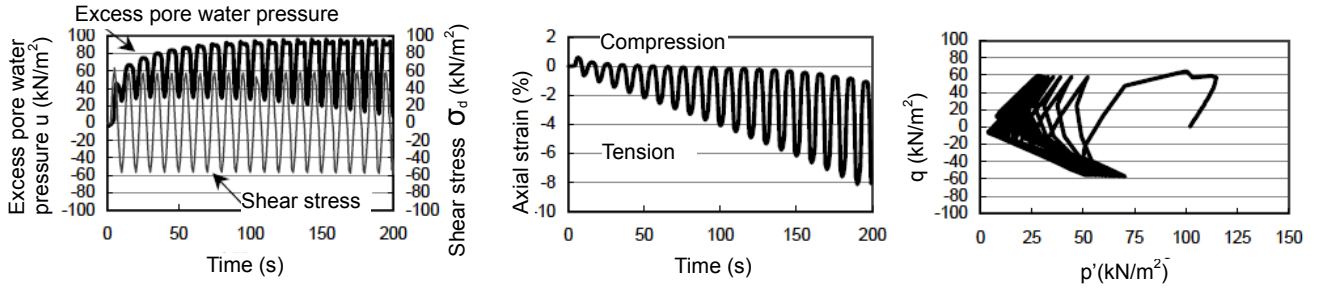

Figure 7 Recorded wave forms for excess pore water pressure, shear stress, axial strain and stress path. (Sample=GBFS B, Dr=50%, $\sigma_d/2\sigma_c$=0.25, φ_d=38.5°, q_u=21.5kN/m^2, CP=28days in alkali water)

In the case that the specimen is under the granular condition, when the double amplitude axial strain DA became 5%, the excess pore water pressure u reached the confining stress (100kPa), as shown in Fig.4.

When a specimen is cured in the tap water for 168 days, a small increase in the unconfined shear strength is seen. However, as shown in Fig.5, the excess pore water pressure u increased up to the confining stress and the liquefaction occurred. As for the axial strain, the deformation of specimen has a tendency to occur to the tension side and it increases more gradually compared with Fig.4. This means that the resistance for liquefaction of

GBFS increases with the curing period in the water. Then, the specimen was easy to be granulated by hands, and this means that the bond force between each particle would be disappeared during cyclic shear.

When the specimen was cured in tap water for 365 days, the unconfined shear strength increased to q_u =126.5kN/m^2. For this specimen, the excess pore water pressure once increased up to about 70% of the confining stress and after that, rather decreased as shown in Fig.6. Then the axial strain increased to a tension side and finally the specimen collapsed showing a crack line on the surface of the specimen between the top of the specimen and the upper pedestal, or on the mid-height of the specimen. This means that specimens are kept solidified to resist the liquefaction and the specimen is considered to be safe for the liquefaction. Similar type of collapse which is induced by cyclic shear stress has been confirmed in the cement stabilized soil.

Fig.7 shows results for the specimen GBFS-B with Dr=50%, which was cured in a highly alkalized and high temperature water. The excess pore water pressure finally reached the effective confining stress. The axial strain, however, shows non-collapse and it is difficult to judge this deformation as a liquefaction. So, in this study, this stage was classified as a transition stage which is located between the liquefaction stage and the non-liquefaction stage.

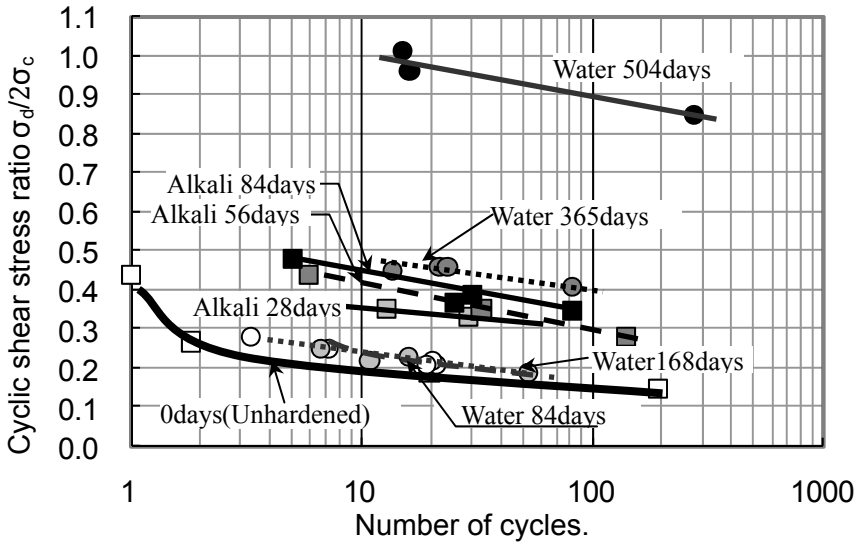

Figure 8 Relationships between cyclic stress ratio and number of cyclic.

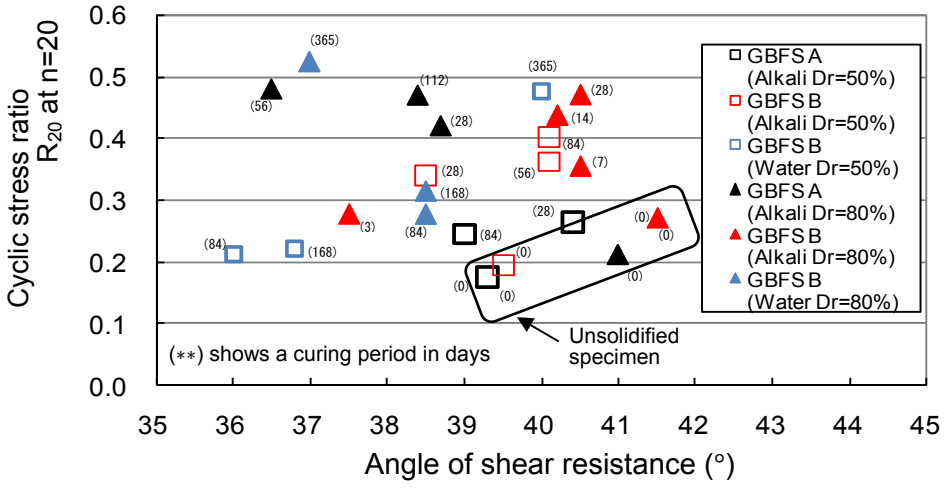

Figure 9 Relationships between the angle of shear resistance and cyclic shear stress ratio R_{20} at n=20.

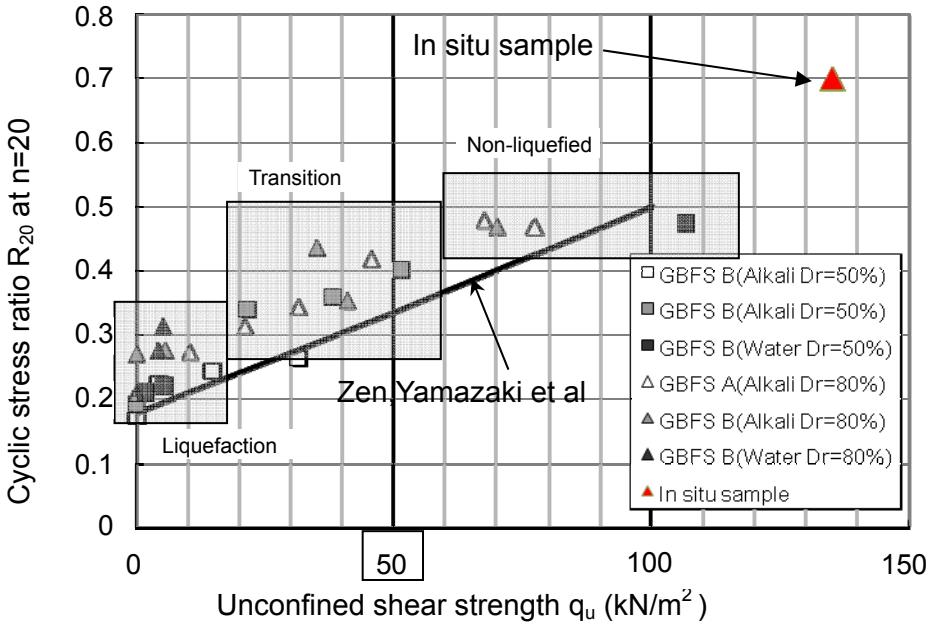

Figure 10 Relationships between cyclic stress ratio R_{20} at n=20 and q_u.

Fig 8 shows relations between cyclic shear stress ratio $\sigma_d/2\sigma_c$ and the number of cycles for GBFS-B with Dr=50%. $\sigma_d/2\sigma_c$ increases with the curing period and when the curing period is 504 days in tap water, $\sigma_d/2\sigma_c$ is showing more than 0.8.

When the cyclic stress ratio R_{20} is defined as the value of $\sigma_d/2\sigma_c$ at the number of cycles n=20, the relationships between R_{20} and the angle of shear resistance are shown in Fig.9. For the un-solidified specimen with no curing in the water, R_{20} increases proportionally with the angle of shear resistance. For specimens, however, cured in the water for a long period of time, no apparent relations are appeared.

As mentioned above, when the specimen is subjected to the cyclic shear under undrained condition, the deformation is divided into three stages which are due to the level of solidification, i.e. liquefaction stage, transition stage and non-liquefied stage. Fig.10 shows the relationships between R_{20} and the unconfined shear strength q_u. R_{20} increases almost lineally with q_u, which is independent of the curing method, Dr and the sample, and when the unconfined shear strength is over 50kN/m^2, the deformation is in the un-liquefied stage. In Fig.10, the results for the cement stabilized soil are also shown, in which the dredged sand and the decomposed granite soil were mixed with cement. Results for GBFS is seen to be larger than those for cement stabilized soil. The plot for the in situ data shown in Fig.10 would be discussed in the next section.

3.2. Comparison between laboratory-prepared sample and in situ sample

To clarify the characteristics of hardening in the field, GBFS was filled in the test site which is located close to the quay wall and the width 6m, the length 8m and the depth 5m. as shown in Fig.11. The undisturbed sample was obtained after curing for 20 months and the unconfined compression tests and also cyclic tri-axial tests were carried out. As shown in Photo 1, GBFS was poured into the test site by a dump truck. After completion of filling GBFS, the standard penetration test was carried out at predetermined curing period. In Fig.12, the changes in the distribution of N-value are shown with time. It is seen that N-value increases with curing period and there is a tendency that the high N-value is seen at the upper layer. After 20 months of curing, N-value at the upper layer reached over 50. At the lower layer, however, N-value is still less than 10. The reason of this small N-value at the lower layer is considered due to the cyclic inflow and outflow of seawater. To confirm the

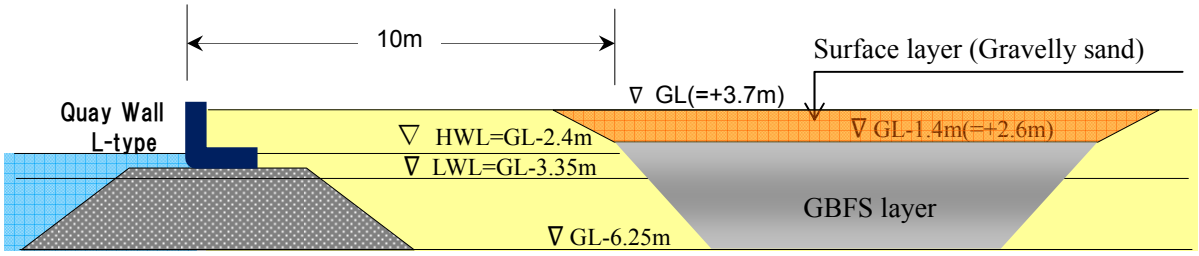

Figure 11 In situ test site.

Photo 1 In situ test site (6mW, 8mL, 5mD) filled with Granulated Blast Furnace Slag.

liquefaction resistance of GBFS, undisturbed sample was obtained by using the triple-tube-sampler. For these undisturbed specimen, unconfined compression tests and also cyclic tri-axial tests were performed. Unconfined compression strength for all samples was in the range from 129 to 141kN/m^2 (average value is135kN/m^2). Fig 13 shows recorded waves for the excess pore water pressure u, cyclic stress σ_d and axial strain. When the excess pore water pressure ratio increased up to 75% of the confined pressure,

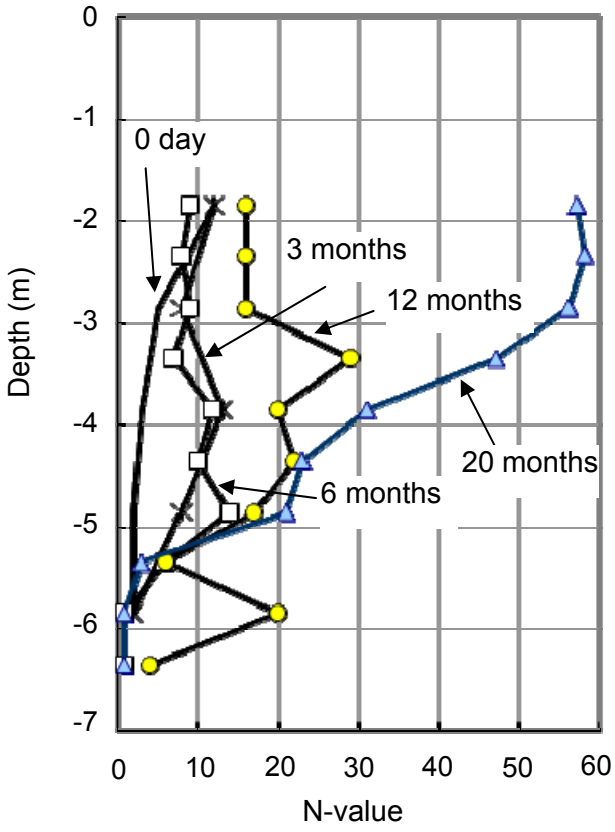

Figure 12 The distribution of N-value and the its change with elapsed time.

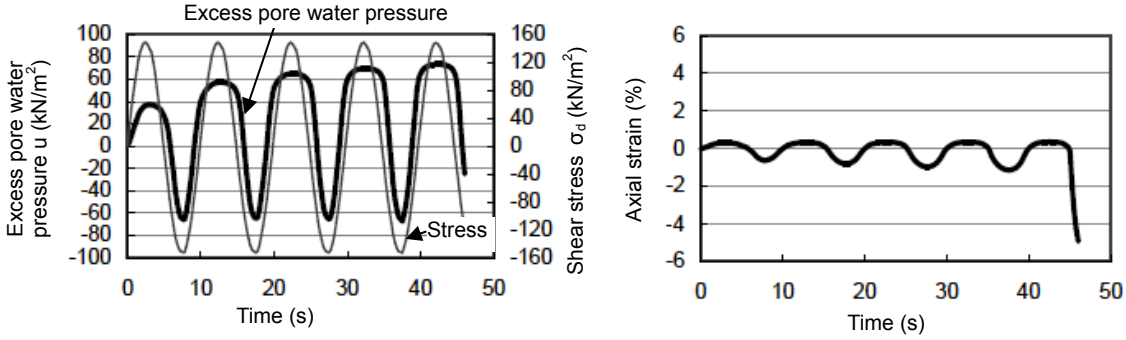

Figure 13 Recorded wave forms for excess pore water pressure, shear stress, and axial strain, for an in situ specimen.

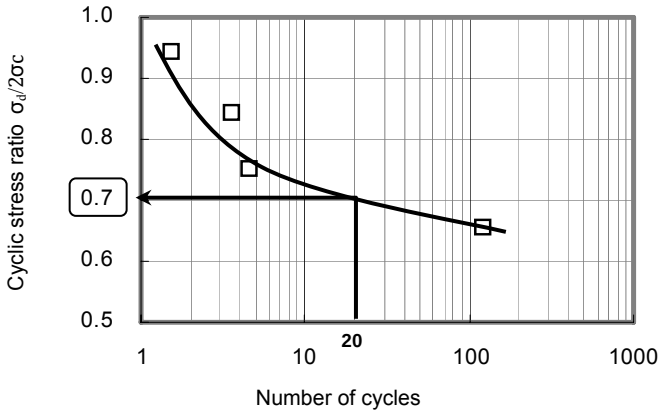

Figure 14 Relationships between number of cycles and cyclic stress ratio for in situ specimens.

the axial strain suddenly increased to a tension side and collapse line was appeared around the mid-height of specimen.

Fig.14 shows relationships between cyclic stress ratio $\sigma_d/2\sigma_c$ and the number of stress cycles. The relationship between R_{20} and the unconfined compression strength for the in situ specimens is shown in the former Fig.10 together with the result for the laboratory prepared specimen. The result for the in situ specimen is on the extrapolated line of the laboratory prepared specimen.

4.CONCLUSIONS

In order to clarify the relations between the degree of hardening and the resistance against the liquefaction, tri-axial compression tests, unconfined compression tests and cyclic un-drained tri-axial tests were carried out for specimens, which were cured in the laboratory and also in situ embankment construction site. The obtained results are as follows.

(1) Cyclic stress ratio R_{20} at n=20 increases linearly with the unconfined compression strength, which is irrespective of the curing method, relative density Dr and type of GBFS.
(2) Cyclic stress ratio R_{20} at n=20 increases with the curing period and when the unconfined compression strength of GBFS is over 50kN/m^2, the liquefaction would not occur.

ACKNOWLEDGEMENTS

In this research, a part of experimental works were performed by the graduate students in Yamaguchi University. The writers would like to express their gratitude to their supports.

REFERENCES

Nippon Slag Association.(2008). *Homepage http://www.slg.jp/*

The Japan Port and Harbour Association. (2007). Technical standards and commentaries for port and harbour facilities. (in Japanese)

Zen, K., Yamazaki, H., Watanabe, A., Yoshizawa H. and Tamai, A. (1987). *Technical note of the port and harbour research institute* **579**, 1-41. (in Japanese)

SHINOZAKI, H., MATSUDA, H. and BAEK, W. (2008). Cyclic shear strength of granulated blast furnace slag in the process of hardening, *JSCE journal of geotechnical and geoenvironmental engineering, Doboku Gakkai Ronbunshuu* C **64, 1,** 175-180. (in Japanese)